Available online at www.sciencedirect.com

SciVerse ScienceDirect

Ceramics International 39 (2013) 3417–3421

CERAMICS INTERNATIONAL

www.elsevier.com/locate/ceramint

Short communication

Clamping characteristics and pulse aging behavior of $ZnO–V_2O_5–Mn_3O_4$ varistor ceramics modified with Nb_2O_5

Choon-W. Nahm*

Semiconductor Ceramics Laboratory, Department of Electrical Engineering, Dongeui University, Busan 614-714, Republic of Korea

Received 20 August 2012; received in revised form 13 September 2012; accepted 14 September 2012
Available online 23 September 2012

Abstract

The clamping characteristics and pulse aging behavior of $ZnO–V_2O_5–Mn_3O_4$ varistor ceramics modified with Nb_2O_5 were investigated at a specified pulse current. The varistor ceramics modified with 0.25 mol% Nb_2O_5 exhibited the best clamp characteristics, in which the clamp voltage ratio is in the range of 1.83–2.57 at a pulse current in the range of 1–50 A. The varistor ceramics modified with 0.05 mol% Nb_2O_5 exhibited the best electrical stability, where $\%\Delta E_{1mA/cm^2} = -2.2\%$ and $\%\Delta\alpha = -30.8\%$ after applying the pulse current of 100 A.

Keywords: A. Sintering; C. Electrical properties; D. ZnO; E. Varistors

1. Introduction

Today, modern electronic systems composed of a lot of semiconductor devices are vulnerable to diverse transient overvoltages. If they do not have a surge protection device (SPD), they will be exposed to dangerous situation. Hence, it is highly desirable to use the so-called varistor (short for variable resistor). The varistor is an electronic component, which exhibits nonlinear *V–I* characteristics. The varistors are generally divided into back-to-back Zener diode and electronic ceramics. The former is a single pn junction diode and has a high nonlinearity and fast response time. The latter is a multi-junction grain boundary device and possesses a much higher energy handling capability than the Zener diode.

Zinc oxide varistors have been widely used to protect various semiconductor devices, electronic circuits, and electric power systems from dangerous abnormal transient voltages due to high energy handling capability as a typical SPD [1,2]. Commercial multilayered chip varistor ceramics are co-fired with an expensive refractory Pd or Pt as an inner-electrode, because they have a desirable sinterability at temperature above 1000 °C. But, $ZnO–V_2O_5$-based ceramics can be co-sintered with a pure Ag as an inner-electrode instead of Pd or Pt because of low sintering temperature of approximately 900 °C [3].

A study on $ZnO–V_2O_5$-based ceramics is in its early stages in many points: materials composition, sintering process, electrical and dielectric properties, stability against DC accelerated aging stress and impulse stress, etc. [4–12]. Up to now, most investigations on $ZnO–V_2O_5$-based varistor ceramics are related to the microstructure and electrical properties in terms of additives and sintering process [7–12]. The electrical stability against a pulse current is technologically the most important factor, which should be considered in the design of ZnO varistor ceramics. However, the surge clamping characteristics and electrical stability against a pulse current in the $ZnO–V_2O_5$-based ceramics have been rarely studied [13,14]. In this work, the effect of Nb_2O_5 on clamping characteristics and pulse aging behaviors of the $ZnO–V_2O_5–Mn_3O_4$ varistor ceramics was investigated and some new results were obtained.

2. Experimental procedure

Reagent-grade raw materials were used in the proportion of $(99.0-x)$ mol% ZnO, 0.5 mol% V_2O_5, 0.5 mol% Mn_3O_4, and x mol% Nb_2O_5 ($x = 0.0$, 0.05, 0.1, and 0.25).

*Tel.: +82 51 890 1669; fax: +82 51 890 1664.
E-mail address: cwnahm@deu.ac.kr

0272-8842/$ - see front matter © 2012 Elsevier Ltd and Techna Group S.r.l. All rights reserved.
http://dx.doi.org/10.1016/j.ceramint.2012.09.052

After milling, the powders were pressed into disk-shaped pellets of 10 mm in diameter and 1.5 mm in thickness at a pressure of 100 MPa. The pellets were set on MgO plate into alumina sagger and sintered at 900 °C in air for 3 h, and furnace-cooled to room temperature. The sintered pellets were lapped and polished. The final pellets were about 8 mm in diameter and 1.0 mm in thickness. Silver paste was coated on both faces of the pellets and the silver electrodes were formed by heating at 550 °C for 10 min. The electrodes were 5 mm in diameter. Finally, after soldering the lead wire to both electrodes, the samples were packaged by dipping them into a thermoplastic resin powder.

The surface microstructure was examined by a scanning electron microscope (FESEM, Quanta 200, FEI, Brno, Czech). The average grain size (d) was determined by the lineal intercept method, given by $d=1.56L/MN$, where L is the random line length on the micrograph, M is the magnification of the micrograph, and N is the number of the grain boundaries intercepted by the lines [15]. The sintered density (ρ) was measured using a density determination kit (238490) attached to balance (AG 245, Mettler Toledo International Inc., Greifensee, Switzerland).

The electric field–current density (E–J) characteristics were measured using a V–I source (Keithley 237, Keithley Instruments Inc., Cleveland, OH, USA). The breakdown field ($E_{1\mathrm{mA/cm^2}}$) was measured at 1.0 mA/cm^2 and the leakage current density (J_L) was measured at $0.8E_{1\mathrm{mA/cm^2}}$. In addition, the nonlinear coefficient (α) is defined by the empirical law, $J=CE^{\alpha}$, where J is the current density, E is the applied electric field, and C is a constant. α was determined in the current density range of 1.0–10 mA/cm^2, where $\alpha=1/(\log E_2-\log E_1)$, and E_1 and E_2 are the electric fields corresponding to 1.0 mA/cm^2 and 10 mA/cm^2, respectively.

The clamping voltage (V_c) was measured at a pulse current (I_p) of 1, 5, 10, 25, and 50 A using a surge generator (Tae-yang Engineering, Busan, Korea) and an oscilloscope (TeK 3020B, Beaverton, Oregon, USA). The pulse current waveform had a width of 20 μs and a rise time of 8 μs. The clamp voltage ratio ($K=V_c/V_{1\,\mathrm{mA}}$) is defined by the ratio of clamping voltage to breakdown voltage. The breakdown voltage ($V_{1\,\mathrm{mA}}$) was measured at a current of 1.0 mA DC. The pulse aging test was performed at a multi-pulse current of 100 A (continuously 3 times for each pulse current) using a surge generator. After applying the pulse current, the V–I characteristics were measured at room temperature.

3. Results and discussion

Fig. 1 shows the SEM micrographs of the samples for different amounts of Nb_2O_5. The average grain size (d) exhibited 6.44, 6.91, 6.64, and 6.67 μm with an increase in the amount of Nb_2O_5. On the whole, the average grain size has a fluctuation [16]. The density of sintered pellets increased slightly from 5.50 to 5.54 g/cm^3 corresponding to 95.1–95.8% of the theoretical density (TD) (pure ZnO, TD = 5.78 g/cm^3) with an increase in the amount of Nb_2O_5 [16].

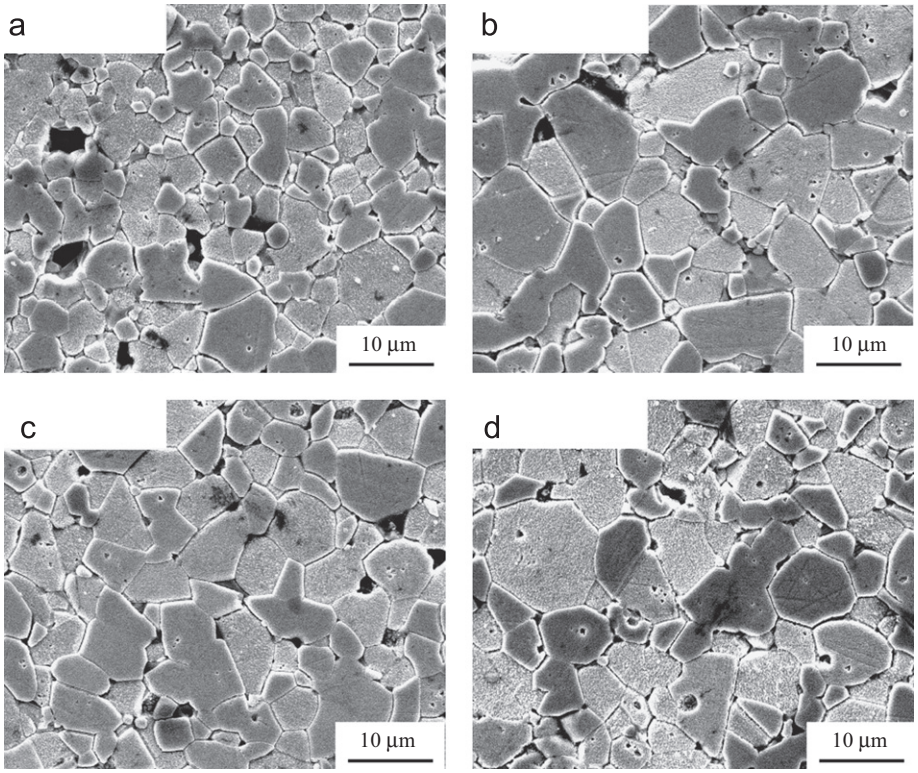

Fig. 1. SEM micrographs of the samples for different amounts of Nb_2O_5: (a) 0.0 mol%, (b) 0.05 mol%, (c) 0.1 mol%, and (d) 0.25 mol%.

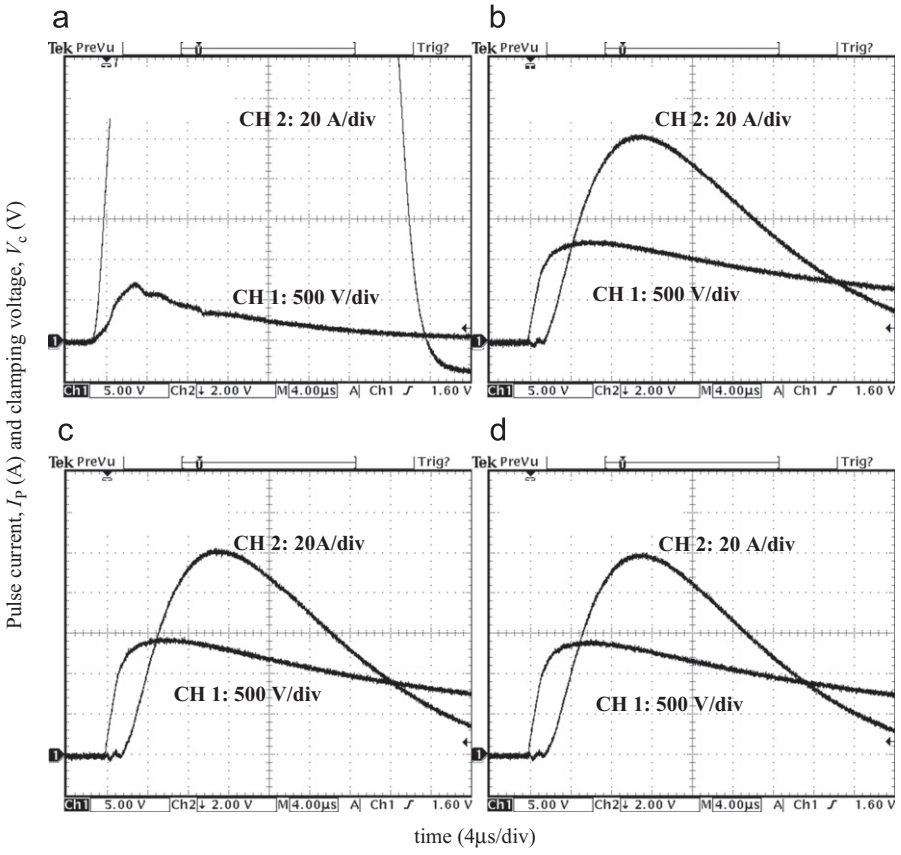

Fig. 2. Clamping voltage waveform for pulse current (100 A) of the samples for different amounts of Nb_2O_5: (a) 0.0 mol%, (b) 0.05 mol%, (c) 0.1 mol%, and (d) 0.25 mol%.

This means the Nb-species may restrict the volatility of the V-species for V_2O_5 with low melting point.

The *E–J* characteristics of the samples for different amounts of Nb_2O_5 are designated as initial in Fig. 3 [16]. It can be seen that the Nb_2O_5 has a noticeable effect on the *E–J* characteristics from the trend of *E–J* curves with an increase in the amount of Nb_2O_5. The initial *E–J* characteristic parameters are summarized in Table 1. The breakdown field (E_{1mA/cm^2}) increased significantly from 1199 to 4544 V/cm up to 0.1 mol% Nb_2O_5. However, further increase in Nb_2O_5 caused E_{1mA/cm^2} to decrease to 4404 V/cm at 0.25 mol%. The behavior of breakdown field (E_{1mA/cm^2}) is directly related to the number of grain boundaries. The nonlinear coefficient (α) increased from 19 to 39 at up to 0.05 mol% Nb_2O_5. However, further increase in Nb_2O_5 caused α to decrease to 15 at 0.25 mol%. The leakage current density (J_L) exhibited the minimum value (0.11 mA/cm^2) at 0.05 mol% Nb_2O_5. Further increase in Nb_2O_5 caused J_L to increase to 0.36 mA/cm^2 at 0.25 mol% Nb_2O_5.

Fig. 2 shows the pulse current (I_p) waveforms of 100 A and clamping voltage (V_c) characteristics in order to investigate a pulse aging behavior for different amounts of Nb_2O_5. But first, the detailed V_c and *K* values corresponding to pulse current of 1–50 A for different amounts of Nb_2O_5 are summarized in Table 1. The V_c is defined by the drop voltage between electrodes of the sample when the specified pulse current flows through the sample. It can be seen that the higher pulse current leads to the higher clamping voltage. The low *K* value means that the varistor ceramics more effectively clamp a pulse current to operating voltage. The sample with no Nb_2O_5 is *K* value as high as 2.60 even at a pulse current of 1 A and the *K* value greatly increased to 5.44 at a pulse current of 50 A. The nonlinearity of this sample is not so bad. Nevertheless the clamping characteristics are not good. In the light of only this result, it seems that this sample exhibits an unstable potential barrier at grain boundaries. On the other hand, the samples modified with Nb_2O_5 exhibited good clamping characteristics, in which the *K* value is less than 2 at a pulse current of 1 A and less than 3 at a pulse current of 50 A. This result indicates that the effect of Nb_2O_5 on clamping characteristics is very noticeable. The sample modified with 0.25 mol% Nb_2O_5 is the best clamping characteristics, in which the *K* value is 1.83–2.57 corresponding to 1–50 A in the pulse current, despite the lowest nonlinear coefficient (15) among the samples. In the light of these results, the highest nonlinear coefficient does not necessarily yield the lowest *K* value.

Fig. 3 compares the variation of *E–J* characteristic curves after applying the higher pulse current of 100 A as indicated in Fig. 2 with the initial *E–J* characteristic for different amounts of Nb_2O_5. The variations of *E–J* characteristics after applying the pulse current stress exhibited a

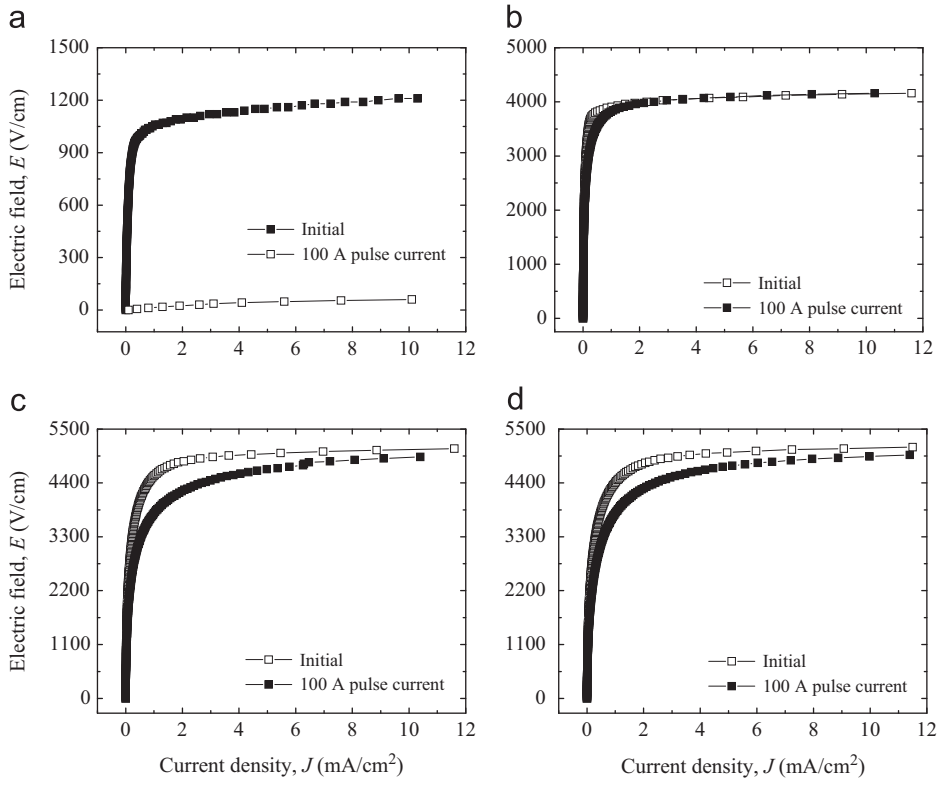

Fig. 3. *E–J* characteristics before and after applying the pulse current of the samples for different amounts of Nb_2O_5: (a) 0.0 mol%, (b) 0.05 mol%, (c) 0.1 mol%, and (d) 0.25 mol%.

Table 1
Breakdown field (E_{1mA/cm^2}), nonlinear coefficient (α), breakdown voltage ($V_{1\,mA}$), clamping voltage (V_c), and clamp voltage ratio (K) of the samples for different amounts of Nb_2O_5.

Nb_2O_5 amount (mol%)	$E_{1\,mA/cm^2}$ (V/cm)	α	$V_{1\,mA}$ (V)	V_c (V)					$K=V_c/V_{1\,mA}$				
				$I_p=1$ A	5 A	10 A	25 A	50 A	$I_p=1$ A	5 A	10 A	25 A	50 A
0.0	1199	19	131	340	460	530	650	710	2.60	3.52	4.06	4.98	5.44
0.05	3909	39	408	740	850	910	1010	1110	1.81	2.08	2.23	2.47	2.72
0.1	4544	21	500	930	1050	1110	1210	1320	1.85	2.10	2.22	2.42	2.64
0.25	4404	15	503	920	1030	1100	1200	1290	1.83	2.05	2.19	2.39	2.57

remarkable difference in accordance with the amount of Nb_2O_5. The sample with no Nb_2O_5 was destroyed after applying the pulse current of 100 A. This sample shows Ohmic behavior in the *E–J* relation as indicated in Fig. 3. The sample modified with 0.05 mol% Nb_2O_5 deviated slightly from initial *E–J* curves after applying the pulse current. This obviously shows that the electrical stability against a pulse current is good. However, the samples modified with 0.1 and 0.25 mol% Nb_2O_5 deviated a little in the vicinity of knee from initial *E–J* curves after applying the pulse current.

The variations of breakdown field ($\%\Delta E_{1mA/cm^2}$), nonlinear coefficient ($\%\Delta\alpha$), and leakage current density ($\%\Delta J_L$) after applying the pulse stress for different amounts of Nb_2O_5 are summarized in Table 2. There is no need to comment on the sample with no Nb_2O_5 which is destroyed after applying the pulse current of 100 A, as mentioned above. However, the sample modified with only 0.05 mol% Nb_2O_5 exhibited -2.2% in the $\%\Delta E_{1mA/cm^2}$. Obviously, this is a surprising effect by the addition of Nb_2O_5. On the other hand, the samples modified with 0.1 and 0.25 mol% Nb_2O_5 exhibited -16.8% and -14.1%, respectively, in the $\%\Delta E_{1mA/cm^2}$ after applying the pulse current of 100 A. They exhibited a relatively low stability for E_{1mA/cm^2} characteristics by recording the variation rates above 10% in $\%\Delta E_{1mA/cm^2}$ after applying the pulse current of 100 A.

The sample modified with 0.05 mol% Nb_2O_5 exhibited variation rate as high as -30.8% in the $\%\Delta\alpha$ after applying the pulse current of 100 A. However, this sample maintained relatively high nonlinear properties by exhibiting an α value of 27 even after applying the pulse current of 100 A. On the contrary, the samples modified with 0.1 and 0.25 mol% Nb_2O_5 exhibited -57.1% and -40%, respectively, in the $\%\Delta\alpha$ after applying the pulse

Table 2
Variation rates of breakdown field ($\%\Delta E_{1mA/cm^2}$), nonlinear coefficient ($\%\Delta\alpha$), and leakage current density ($\%\Delta J_L$) before and after applying the pulse current of the samples for different amounts of Nb_2O_5.

Nb_2O_5 amount (mol%)	Pulse current (A)	E_{1mA/cm^2} (V/cm)	$\%\Delta E_{1mA/cm^2}$	α	$\%\Delta\alpha$	J_L (mA/cm^2)	$\%\Delta J_L$
0.0	Initial	1199	–	19	–	0.18	–
	100 (3 times)	22	−98.2	1.5	−92.1	0.74	311.1
0.05	Initial	3909	–	39	–	0.11	–
	100 (3 times)	3824	−2.2	27	−30.8	0.34	209.1
0.1	Initial	4544	–	21		0.32	–
	100 (3 times)	3780	−16.8	9	−57.1	0.34	6.2
0.25	Initial	4404	–	15	–	0.36	–
	100 (3 times)	3783	−14.1	9	−40.0	0.43	19.4

current of 100 A. They exhibited a relatively low stability for α characteristics by recording α less than 10 after applying the pulse current of 100 A. On the whole, the $ZnO–V_2O_5–Mn_3O_4$ varistor ceramics modified with 0.05 mol% Nb_2O_5 have relatively good varistor characteristics at a pulse current of 100 A.

4. Conclusions

The effect of Nb_2O_5 on claming characteristics and pulse aging behavior of the $ZnO–V_2O_5–Mn_3O_4$ varistor ceramics was investigated. The Nb_2O_5 did have a noticeable effect on clamp ratio, which exhibits a surge protection capability. The varistor ceramics modified with 0.25 mol% Nb_2O_5 exhibited the best clamp characteristics by exhibiting the lowest clamp voltage ratio (K) at a pulse current of 1–50 A. The varistor ceramics modified with 0.05 mol% Nb_2O_5 exhibited the highest electrical stability, with $\%\Delta E_{1mA/cm^2} = -2.2\%$, and $\%\Delta\alpha = -30.8\%$ after applying the pulse current of 100 A. Conclusively, the amount of Nb_2O_5 is optimized at 0.05 mol% based on nonlinearity, clamping characteristics, and surge absorption capability.

References

[1] L.M. Levinson, H.R. Philipp, Zinc oxide varistor—a review, American Ceramic Society Bulletin 65 (1986) 639–646.
[2] T.K. Gupta, Application of zinc oxide varistor, Journal of the American Ceramic Society 73 (1990) 1817–1840.
[3] J.-K. Tsai, T.-B. Wu, Non-ohmic characteristics of $ZnO–V_2O_5$ ceramics, Journal of Applied Physics 76 (1994) 4817–4822.
[4] J.-K. Tsai, T.-B. Wu, Microstructure and nonohmic properties of binary $ZnO–V_2O_5$ ceramics sintered at 900 °C, Materials Letters 26 (1996) 199–203.
[5] C.T. Kuo, C.S. Chen, I.-N. Lin, Microstructure and nonlinear properties of microwave-sintered $ZnO–V_2O_5$ varistors: I, effect of V_2O_5 doping, Journal of the American Ceramic Society 81 (1998) 2942–2948.
[6] H.-H. Hng, K.M. Knowles, Microstructure and current–voltage characteristics of multcomponent vanadium-doped zinc oxide varistors, Journal of the American Ceramic Society 83 (2000) 2455–2462.
[7] H.-H. Hng, P.L Chan, Effects of MnO_2 doping in V_2O_5-doped ZnO varistor system, Materials Chemistry and Physics 75 (2002) 61–66.
[8] H.-H. Hng, P.L Chan, Microstructure and current–voltage characteristics of $ZnO–V_2O_5–MnO_2$ varistor system, Ceramics International 30 (2004) 1647–1653.
[9] C.-W. Nahm, Effect of sintering temperature on varistor properties and aging characteristics of $ZnO–V_2O_5–MnO_2$ ceramics, Ceramics International 35 (2009) 2679–2685.
[10] C.-W. Nahm, Preparation and varistor properties of new quaternary Zn–V–Mn–(La, Dy) ceramics, Ceramics International 35 (2009) 3435–3440.
[11] C.-W. Nahm, Effect of dopant (Al, Nb, Bi, La) on varistor properties of $ZnO–V_2O_5–MnO_2–Co_3O_4–Dy_2O_3$ ceramics, Ceramics International 36 (2010) 1109–1115.
[12] C.-W. Nahm, Varistor properties and aging behavior of $ZnO–V_2O_5–Mn_3O_4$ ceramics with sintering process, Journal of Materials Science: Materials in Electronics 22 (2011) 1010–1015.
[13] C.-W. Nahm, Impulse aging behavior of $ZnO–V_2O_5$-based varistors with Nb_2O_5 addition, Journal of the American Ceramic Society 94 (2011) 1305–1308.
[14] C.-W. Nahm, Sintering effect on pulse aging behavior of Zn–V–Mn–Co–Dy–Nb varistors, Journal of the American Ceramic Society 94 (2011) 2269–2272.
[15] J.C. Wurst, J.A. Nelson, Lineal intercept technique for measuring grain size in two-phase polycrystalline ceramics, Journal of the American Ceramic Society 55 (1972) 109–111.
[16] C.-W. Nahm, Nb_2O_5 doping effect on electrical properties of $ZnO–V_2O_5–Mn_3O_4$ varistor ceramics, Ceramics International 38 (2012) 5281–5285.